

Prediction Unconfined Compressive Strength for Different Lithology Using Various Wireline Type and Core Data for Southern Iraqi Field

Worood Al-Zubaidy^{1,*}, Mohammed Al-Jawad²

Department of Petroleum Engineering, College of Engineering, University of Baghdad, Baghdad, Iraq
engineerworood1989@gmail.com¹, mjawad@coeng.uobaghdad.edu.iq²

ABSTRACT

Unconfined Compressive Strength is considered the most important parameter of rock strength properties affecting the rock failure criteria. Various research have developed rock strength for specific lithology to estimate high-accuracy value without a core. Previous analyses did not account for the formation's numerous lithologies and interbedded layers. The main aim of the present study is to select the suitable correlation to predict the UCS for hole depth of formation without separating the lithology. Furthermore, the second aim is to detect an adequate input parameter among set wireline to determine the UCS by using data of three wells along ten formations (Tanuma, Khasib, Mishrif, Rumaila, Ahmady, Maudud, Nahr Umr, Shuaiba and Zubair). After calibration with core test, the results revealed that Young's Modulus correlations are the best to predict UCS with RMSE (53.23 psi). Furthermore, the result showed that using the static Young Modulus as an input parameter in predicting UCS gives a closer result to the laboratory test than using a sonic log. This study found that many previous equations were developed for only one type of rock and tended to generalize poorly to the broader database. This study also provided more accurate rock strength estimation, leading to better prognosis in operational strategies and hydraulic fracturing location planning in oil well development when geomechanical analysis needs to be addressed where no core is available. Finally, the expected continuous rock mechanical profile indicates the formation's strength and stability around the wellbore.

Keywords: Un-confined compressive strength, Lithology, Wireline, Core data.

*Corresponding author

Peer review under the responsibility of University of Baghdad.

<https://doi.org/10.31026/j.eng.2023.11.07>

This is an open access article under the CC BY 4 license (<http://creativecommons.org/licenses/by/4.0/>).

Article received: 09/03/2023

Article accepted: 13 /04/2023

Article published: 01/11/2023

التنبؤ بقوة الانضغاط غير المحصورة لأنواع مختلفة من الصخور باستخدام مجسات متنوعة وفحوصات اللباب لحقل في جنوب العراق

ورود عبد العباس حسن^{1*}، محمد صالح الجواد²

قسم هندسة النفط، كلية الهندسة، جامعة بغداد، بغداد، العراق

الخلاصة

تعتبر قوة الانضغاط الغير محصورة من اهم خصائص مقاومة الصخور التي تؤثر على معيار انهيار الصخور. اجريت العديد من الدراسات لتطوير التنبؤ بتلك الخاصية والحصول على حسابات دقيقة في غياب الفحوصات المختبرية. الدراسات السابقة كانت تتناول نوع محدد من الصخور ولم تأخذ بنظر الاعتبار ان التكوينات الجيولوجية تكون معقدة التركيب وتتألف من عدة انواع من الصخور التي تكون غالبا متداخلة مع بعضها بشكل طبقات متتابعة يصعب فصلها. الهدف الاساسي من هذه الدراسة هو تحديد المعادلة المناسبة لحساب قوة الانضغاط الغير محصورة للعمق الكامل للتكوين بإهمال نوع الصخرة، بالإضافة الى ذلك تحديد اي نوع من المجسات او الخواص الميكانيكية التي تعطي تنبؤ جيد لقوة الانضغاط الغير محصورة باستخدام بيانات ثلاث آبار ولعشرة تكوينات (تنومه، الخصيب، المشرف، الرميلة، الأحمدى، مودود، نهر عمر، الشعبية، الزبير). اظهرت النتائج وبعد المطابقة مع الفحوصات المختبرية ان معادلة يونك هي الأكثر واقعية واعطت مقدار خطأ حوالي (53.23 psi)، بالإضافة الى ذلك فأن استخدام معامل يونك لحساب قوة الانضغاط الغير محصورة هو الاقرب من القيم المختبرية على العكس من استخدام مجسات سرعة الصوت التي اعطت قيم بعيدة جدا.

في هذه الدراسة وجد ان العديد من المعادلات السابقة تم تطويرها لنوع محدد من الصخور وعند استخدامها للتعميم سوف تعطي نتائج خاطئة. قدمت هذه الدراسة ايضا تقدير اكثر دقة لقوة الصخور مما يؤدي الى تشخيص افضل في الاستراتيجيات التشغيلية وتخطيط موقع التكسير الهيدروليكي في تطوير آبار النفط عندما يحتاج النموذج الجيوميكانيكي الى معالجه عند عدم توفر الفحوصات المختبرية. واخيرا فأن ايجاد العمود المستمر للخواص الصخرية يعتبر مؤشر جيد لقوة واستقرار التكوين حول جدار البئر.

الكلمات المفتاحية: قوة الانضغاط غير المحصورة، نوع الصخرة، مجسات تخطيط الآبار، بيانات اللباب.

1. INTRODUCTION

The Uniaxial Compressive Strength (UCS) and elastic characteristics of rocks, such as Young's modulus and Poisson's ratio, are extensively used to estimate in situ stresses, wellbore stability study, reservoir compaction survey, and prediction of optimal drilling mud pressure (Chang et al., 2006; Abdulraheem et al., 2009). Rocks' Elastic characteristics are assessed using dynamic and static techniques, while UCS is exclusively determined using the static technique (Al-Shayea, 2004) and core test. In the dynamic technique, compressional and shear wave velocities may be recorded in the lab or the field, and elastic characteristics can be computed appropriately. Empirical correlations have been presented to solve the



problem of inferring mechanical parameters from wireline data (**Edimann et al., 1998; Ameen et al., 2009; Ranjbar-Karami and Shiri, 2014**). These correlations estimate porosities or acoustic velocities by empirically correlating laboratory-derived rock mechanical characteristics with geophysical well logs (**Hassan and Hussien, 2019**). Many elements that impact rock mechanical characteristics also affect porosity, velocity, and elastic moduli underlies these correlations (**Chang et al., 2006**). To predict the UCS value when no core is available for laboratory testing, several notable previous publications studied the relationship between the UCS with the well log properties for specific formations and geological settings, creating different UCS equations at specific settings (**Abed and Hamd-Allah, 2019; Aziz and Hussein, 2021a; Aziz and Hussein, 2021b**). Many empirical correlations estimate rock mechanical characteristics using geophysical logging data (**Ryshkewitch, 1953**). Case studies of geological features globally yielded these connections. Rock mechanical profiles may be accurately and efficiently obtained by correlating porosity with several rock mechanical characteristics. According to (**Hoshino, 1974**) rock strength and elasticity depend on porosity. (**Kowalski, 1975; Sethi, 1981**) proposed porosity wireline logs for rock strength parameters. (**Vernik et al., 1993**) calculated unconfined compressive strength from porosity for sedimentary basins globally, especially for highly clean, well-consolidated sandstones with porosity < 0.3. (**Sarda et al., 1993**) identified a straightforward empirical relationship between rock porosity and unconfined compressive strength. The relationship was discovered using laboratory research on sandstone core samples from the Germigny-sous-Coulombs structure in France. (**Edimann et al., 1998**) employed core-measured porosity and rock mechanical parameters for North Sea sandstone samples to determine direct linear correlations between them and estimate the continuous rock mechanical profile. (**Horsrud, 2001**) used the power law function to suggest North Sea Tertiary shale transit time and UCS connection. (**Chang et al., 2006**) synthesized UCS and acoustic transit time data for worldwide, Gulf of Mexico, and Pliocene and younger shale. (**Onyia, 1988**) estimated the UCS from well logs for shale, sandstone, limestone, dolomite, granite, and mixed lithologies. (**Horsrud, 2001**) developed the UCS estimation from compressional wave velocity for the North Sea area. Hareland and Nygaard (2007) developed the equation for calculating the UCS from sonic transit time for sandstone, shale, and mixed lithologies for onshore United Kingdom, offshore North Sea, and Norwegian Sea. The studied interval passes through complex formations (these formation contain limestone, dolomite, sandstone interbedded with beds of shale. The main advantage of the present study is to find suitable correlation to predict the UCS for longer well section, then, the operational cost can be decreased by minimizing the need to conduct core operations and laboratory measurements.

In this study, many previous correlations are applied to the data of the three wells. Then, the results are calibrated with the core data. Finally, statistical analysis is done to detect the suitable correlation to get a good match with laboratory tests and can be used to estimate the UCS for the total depth of complex formations regardless of the lithology.



2. AVAILABLE DATA

All data in this work are collected from the Southern Iraqi oilfield. The data includes geophysical logging and mechanical properties and focuses on formations consisting of complex lithology (ex, shale interbedded with sandstone or limestone)(Neemay and Selman, 2020). The lithology description for studied wells is illustrated in Fig. 1, while Fig. 2 to 4 describes the available logs for each well.

Period	Age		Group	Formation	Lithology	Description	Average thickness (m)	
	Epoch							
Tertiary	L. Miocene-Recent	Kuwait	Dibdibba	[Sand & pebble pattern]	Sand & pebble	200		
			Lower fars	[Clay St, Lst arg pattern]	Clay St, Lst arg	170		
			Ghar	[Sand & subround pebble occ Clay pattern]	Sand & subround pebble occ Clay	110		
	M-L Eocene	Hasa	Dammam	[Dolomite, porous vuggy pattern]	Dolomite, porous vuggy	210		
			Rus	[Anhydrite, white, massive Interbedded w\ Dolomite pattern]	Anhydrite, white, massive Interbedded w\ Dolomite	165		
	Cretaceous	Paleocene -Early Eocene	Aruma	Umm-Er-Radhuma	[Dolomite grey saccharoidol, inpart anhydritic pattern]	Dolomite grey saccharoidol, inpart anhydritic	450	
				Tayarat	[Bituminous Shale at top, Dolomite, grey pattern]	Bituminous Shale at top, Dolomite, grey	220	
				Shiranish	[Limestone marly pattern]	Limestone marly	120	
				Hartha	[Lst, gloc, Dol, porous, locally vuggy, Lst, grey, arg. pattern]	Lst, gloc, Dol, porous, locally vuggy, Lst, grey, arg.	180	
				Sadi	[Limestone white, chalky, fine, compact pattern]	Limestone white, chalky, fine, compact	260	
Tanuma				[Shale: black-brown fissile pattern]	Shale: black-brown fissile	50		
Khasib				[Limestone: grey shaly pattern]	Limestone: grey shaly	45		
Middle Cretaceous				Wasia	Mishrif	[Limestone: white detrital, porous, rudist pattern]	Limestone: white detrital, porous, rudist	150
					Rumaila	[Limestone: grey, marly pattern]	Limestone: grey, marly	100
					Ahmadi	[Shale: Dark grey, fissile w/ Limestone: grey pattern]	Shale: Dark grey, fissile w/ Limestone: grey	140
	Mauddud	[Limestone grey pattern]	Limestone grey		110			
	Nahr Umr	[Shale black inter. w/ Sst pattern]	Shale black inter. w/ Sst		270			
Early Cretaceous	Thamama	Shuaiba	[Lst, Dolomite fracture pattern]	Lst, Dolomite fracture	85			
		Zubair	[Shale, fissile, w/ sandstone fine-m. grained, Silt st, Clay st. pattern]	Shale, fissile, w/ sandstone fine-m. grained, Silt st, Clay st.	400			
		Ratawi	[Limestone with streaks of Shale pattern]	Limestone with streaks of Shale	200			
		Yamama	[Limestone, light grey pattern]	Limestone, light grey	120			
		Jurassic	Upper Jurassic		Sulaiy	[Limestone, argillaceous and marly pattern]	Limestone, argillaceous and marly	300

Figure 1. Lithology description for Southern Iraqi Fields (INOC, 1979)



In this study, three wells are used for UCS prediction analysis, these are X1, X2, and X3. There are core tests available in Tanumma, Mishrif, Nahr Umr, and Zubair formations. **Table 1.** Summarizes the well data used in this study.

Table 1. Well data summary.

Well Name	Data				
	Well Logs			Static Rock Properties	Core Data
	Density Log	Sonic Log	Effective Porosity		
X1	Available	Available	Available	Not Available	Available
X2	Available	Available	Available	Not Available	Available
X3	Available	Available	Available	Not Available	Available

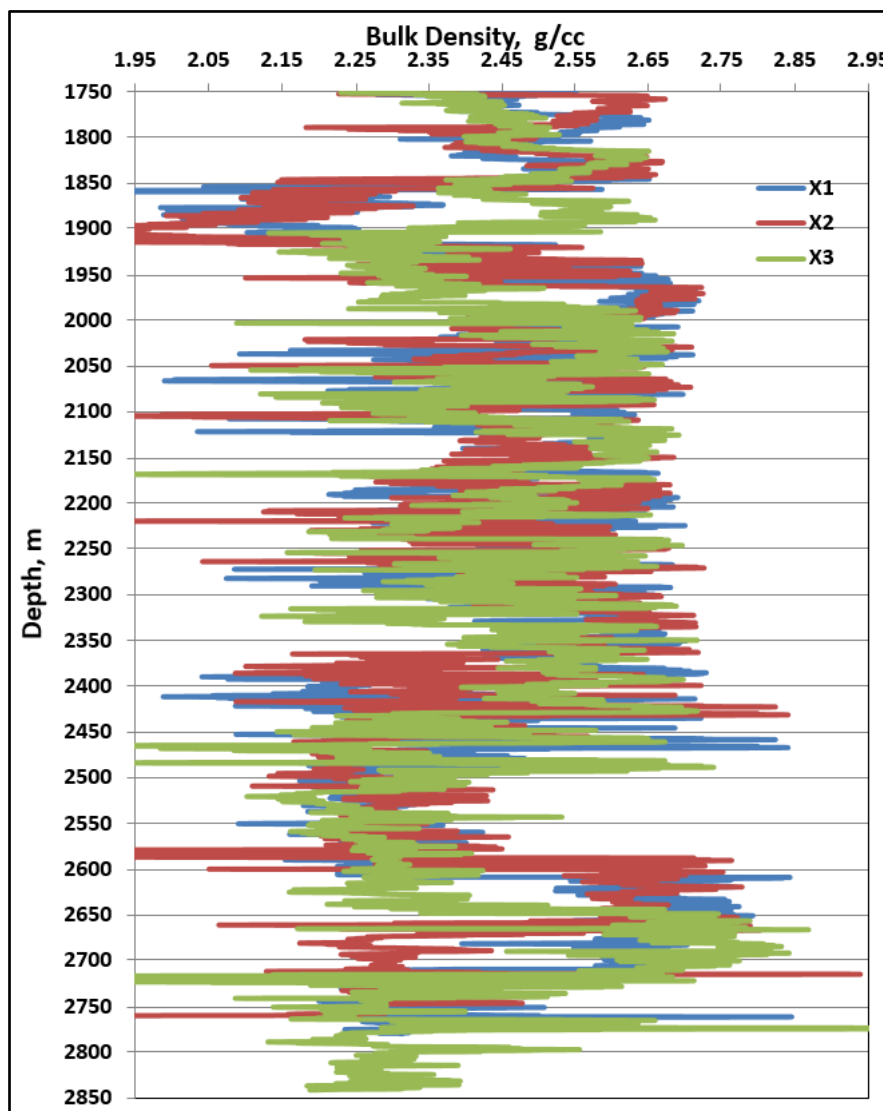


Figure 2. Bulk density graph for studied wells.

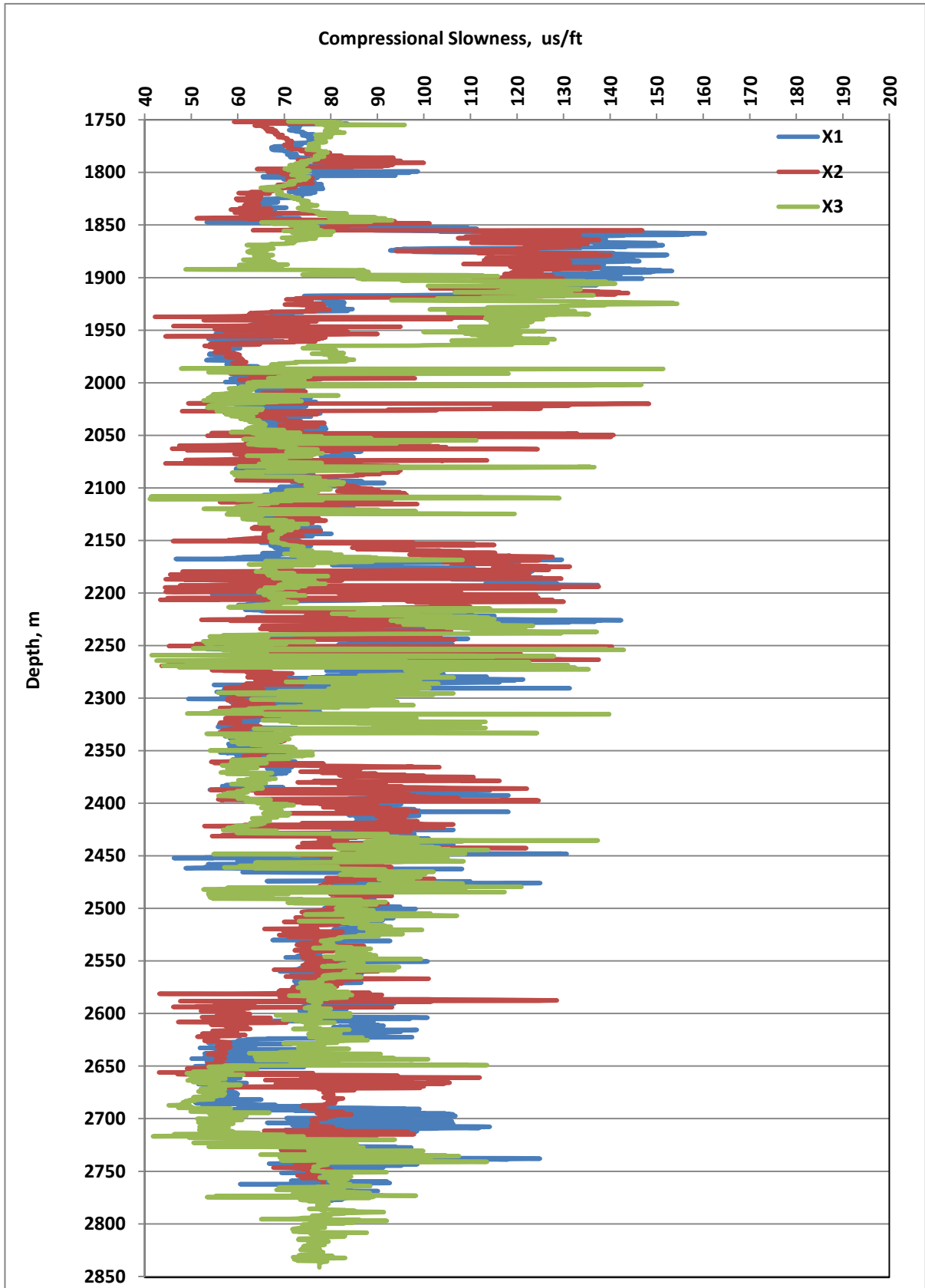


Figure 3. Compressional Wave Velocity for studied wells.

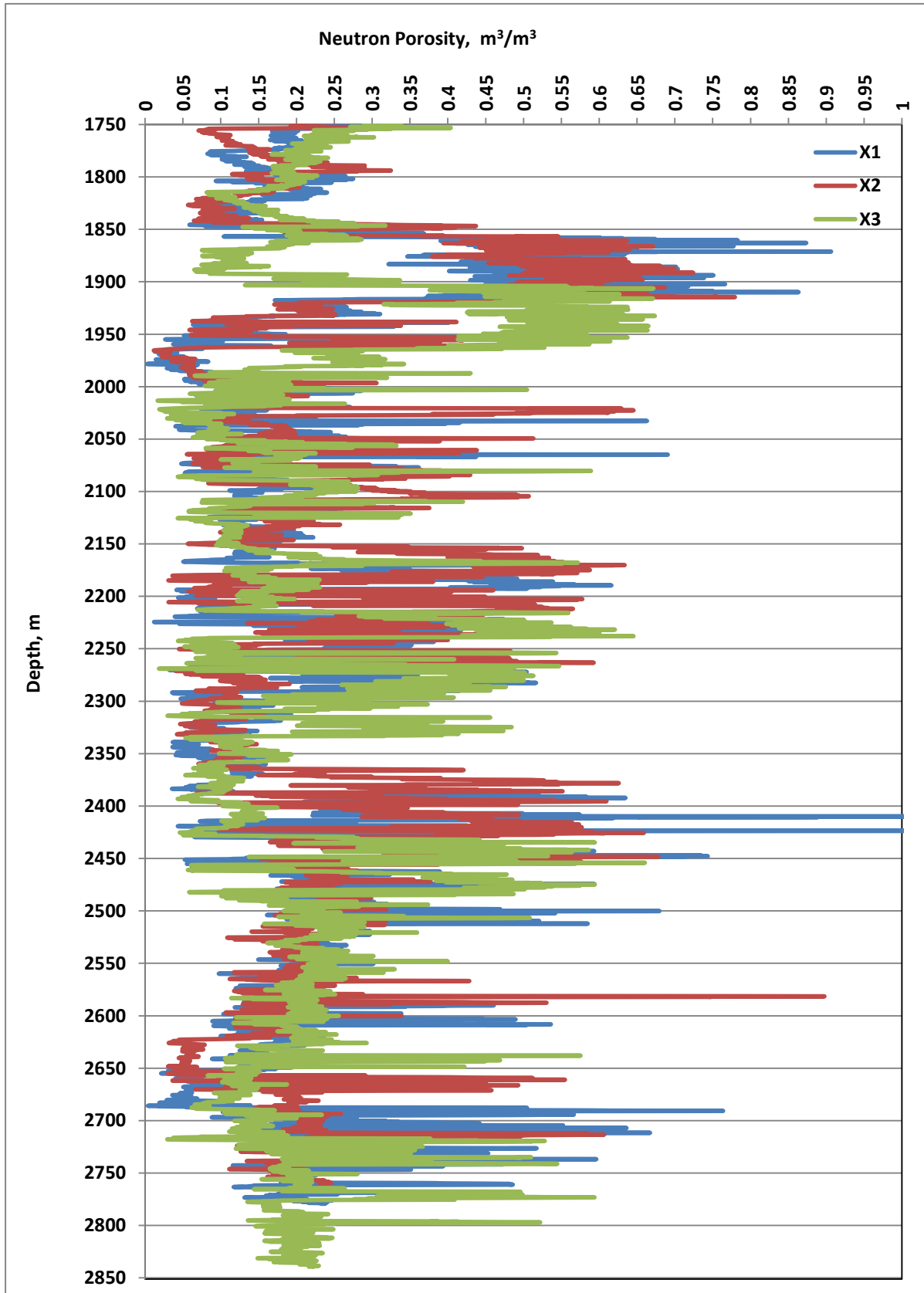


Figure 4. Neutron Porosity graph for studied wells.

3. METHODOLOGY

- Following the identification of all essential and usable data files, non-ASCII files were changed to ASCII files utilizing free software.
 - The next step was to create a plot of the data to assess its accuracy.
 - Once the log data has been loaded, rock may start doing property calculations.
 - Estimate Dynamic and Static Young's Modulus.
 - Several models have been investigated to predict UCS by using Excel program (**Coates Denoo, 1963; McNally, 1987; Vernik et al., 1993; Plumb, 1994; Bradford et al., 1998; Moos et al., 2003; static Young's, 2002; Savitri et al., 2021**).
 - Calibration has been performed between the results and lab test data.
 - Statistical analysis was used to detect which correlation gives a good match with core test.
- Flowchart for building the model using Excel illustrated in **Fig. 5**.

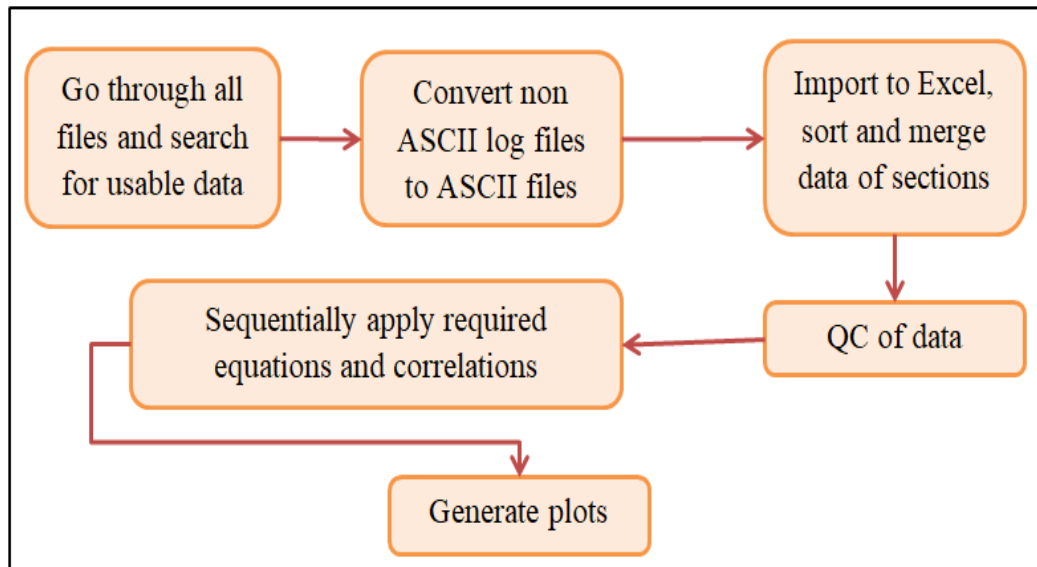


Figure 5. Flowchart for building the model using Excel.

4. RESULT AND DISCUSSION

4.1 Determination of Dynamic and Static Young's Modulus

Young's modulus is the stiffness degree of the rock (**Fjær et al., 2021; Ahmed and Al-Jawad, 2020**). Hooke's law defines the rules for the linear relationship that exists between stress (σ) and strain (ϵ) (**Allawi and Al-Jawad, 2021a**). Some correlations to predict UCS depend on Young's Modulus, so the equations below are applied to predict the Young Modulus value. **Figs. 6 to 8** illustrate the results of Static Young's Modulus, which was calculated by Eq. 2 and appears to match laboratory tests.

$$E_{dyn} = \frac{9G_{dyn}K_{dyn}}{G_{dyn} + 3K_{dyn}} \quad (1)$$



$$E_{static} = 0.032 \times E_{dyn}^{1.632}$$

(2)

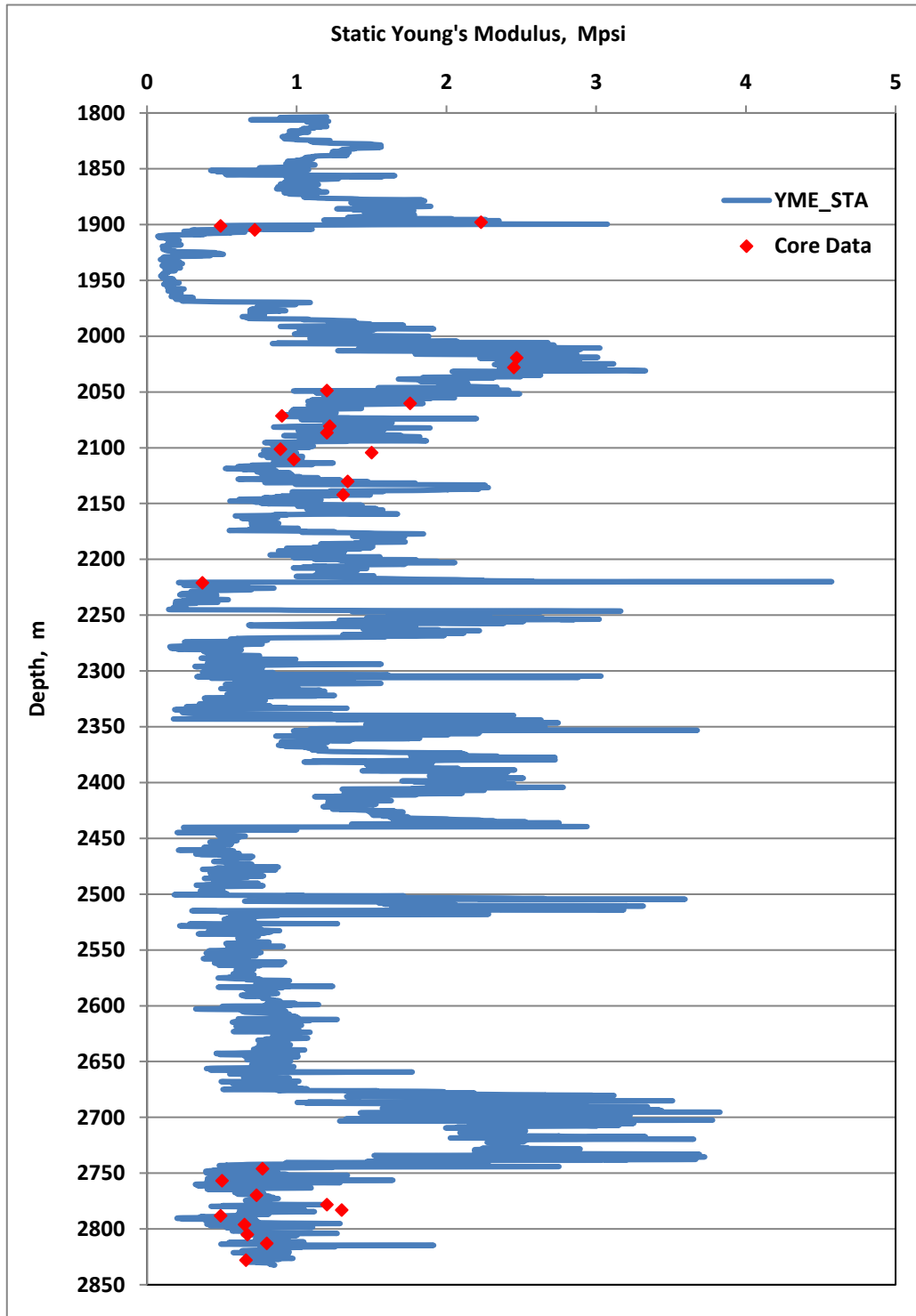


Figure 6. Static Young Modulus for well X1.



where:

$$G_{dyn} = 13474.45 \frac{\rho_b}{(\Delta t_s)^2} \tag{3}$$

$$K_{dyn} = 13474.45 \frac{\rho_b}{(\Delta t_c)^2} - \frac{4}{3} G_{dyn} \tag{4}$$

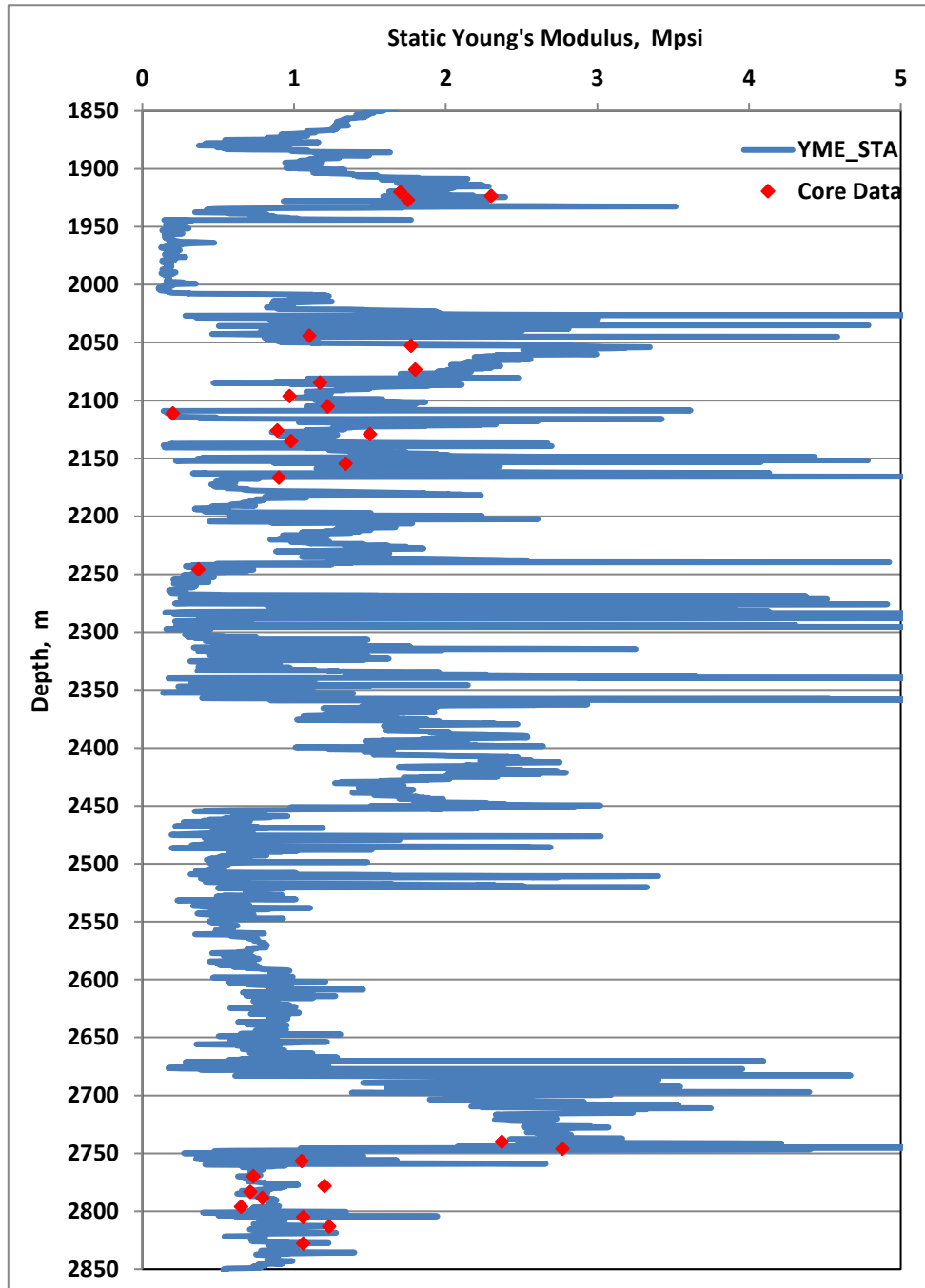


Figure 7. Static Young Modulus for well X2.

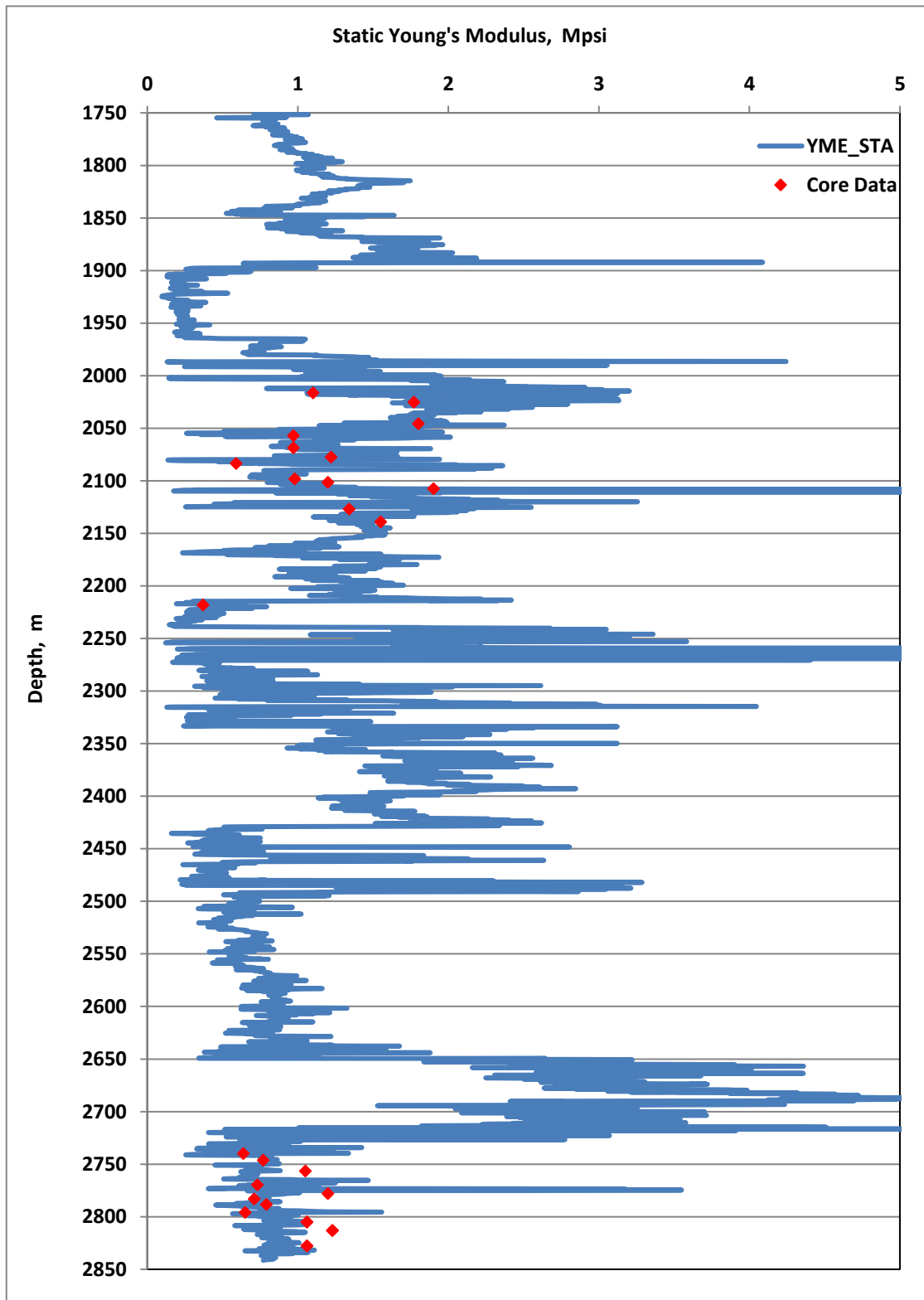


Figure 8. Static Young Modulus for well X3.



4.2 Determination of UCS

The un-confined compressive strength significantly affects wellbore stability because it is a vigorous player determining the failure criterion (Allawi and Al-Jawad, 2021b). Therefore, compressive strength estimation should be accurate because it is the final word on the eventual calculations (Xu et al., 2016). To get better results and avoid obstacles, several models have been investigated. Table 2 shows these correlations with the results of statistical analysis (RMSE), where the results showed a significant difference between the Young Modulus correlation and other correlations, the reason is due to the dependence of the Young Modulus correlation on E_s and it is non-limitation by shally formations . After that the laboratory test data is compared with the results, as presented in Figs. 9 to 12.

Table 2. Various published correlations to calculate the UCS.

Equation for UCS	Reference	Root Mean Square Error (RMSE, psi)	Remarks
$UCS = 0.0866 * \frac{E_{dyn}}{C_{dyn}} [0.008V_{sh} + 0.0045(1 - V_{sh})]$	(Coates Denoo, 1963)	1767.545201	
$UCS = 1200e^{(-0.036\Delta t_c)}$	(McNally, 1987)	6021.376747	Australia
$UCS = 1.4138 * 10^7 \Delta t_c^{-3}$	(McNally, 1987)	765.875069	Gulf Coast
$UCS = 254(1 - 2.8\phi)^2$	(Vernik et al., 1993)	5847.594145	
$UCS = (2.28 + 4.1089E_s) * 145.037$	(Bradford et al., 1998)	229.3667259	
$UCS = (4.242 + E_s) * 145.037$	(Yme, 2002)	53.23181247	
$UCS = (46.2e^{0.0247E_s}) * 145.037$	(Moos et al., 2003)	4757.76922	
$UCS = 0.9616\Delta t_c^2 - 136.5\Delta t_c + 5002$	(Novel et al., 2021)	164965.9605	Shale Gas, Lithology neglecting
$UCS = 0.2686\Delta t_c^2 - 50\Delta t_c + 2339$	(Novel et al., 2021)	14967.9491	Shale Gas, Lithology considering
<i>Where:</i> $C_{dyn} = \frac{1}{K_{dyn}}$ $UCS = psi ; E_s = GPa ; \Delta t_c = us/ft ; E_{dyn} = psi ; K_{dyn} = psi$			

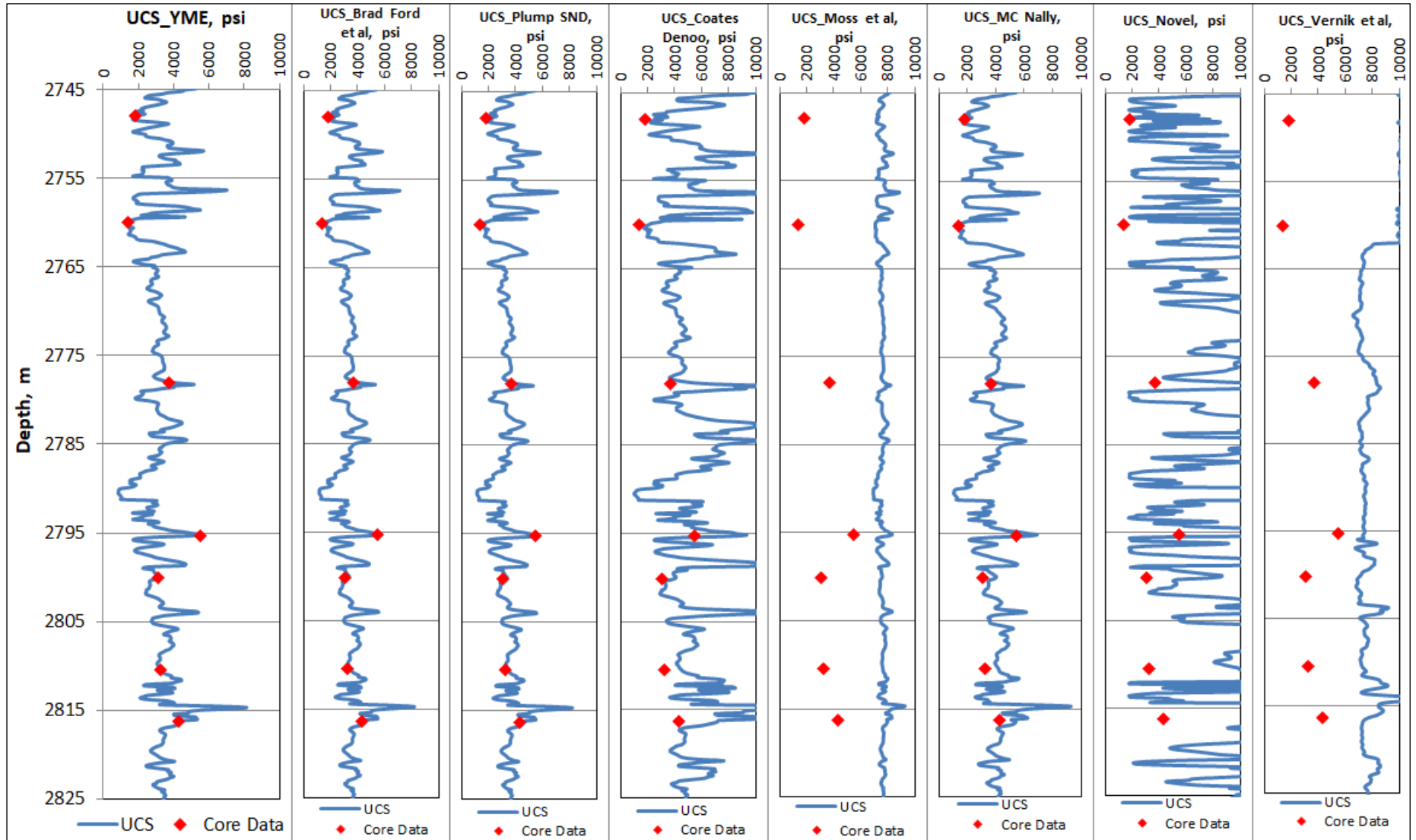


Figure 9. Unconfined compressive strength zmeasured by several methods for well X1.

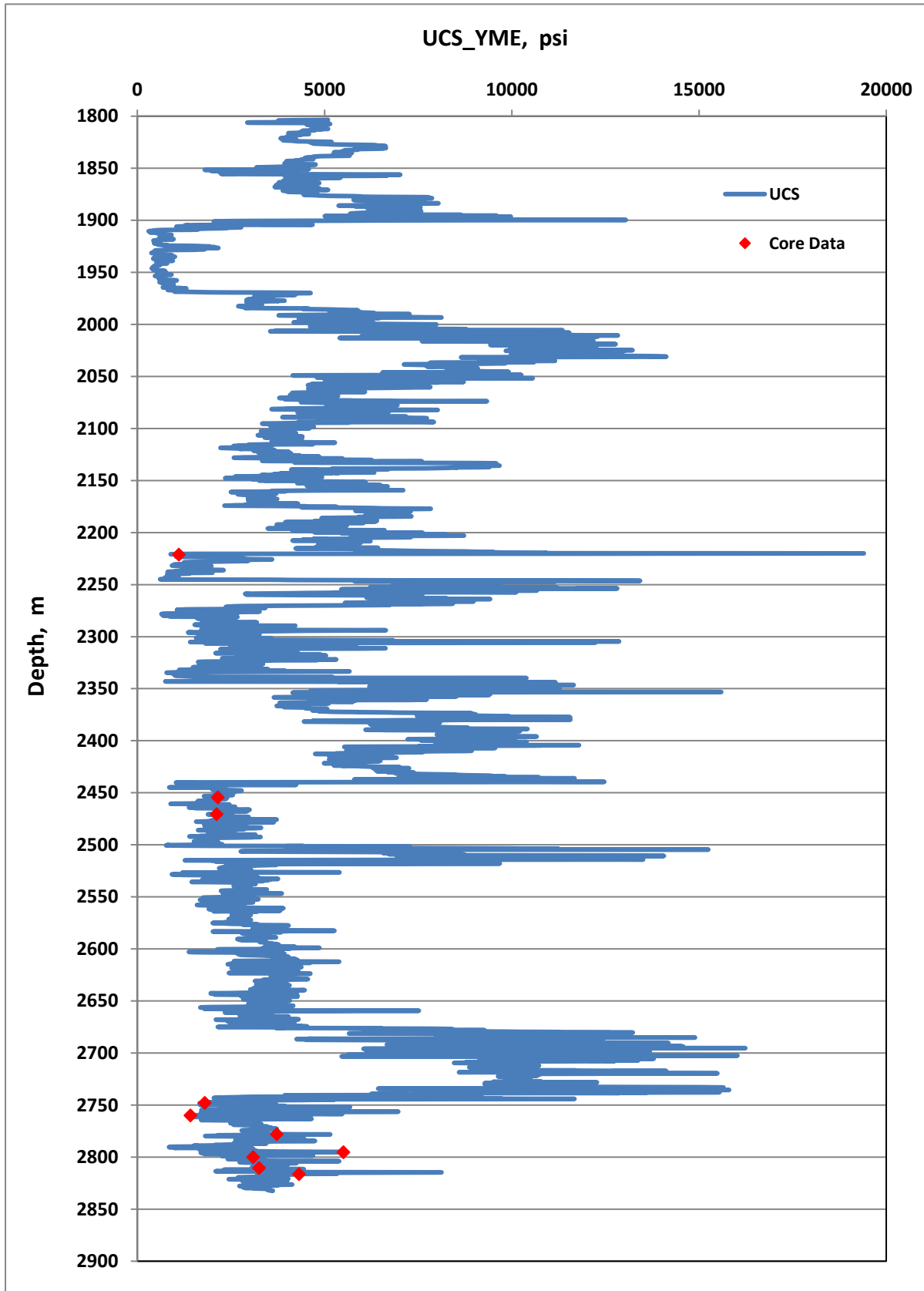


Figure 10. UCS for well X1.

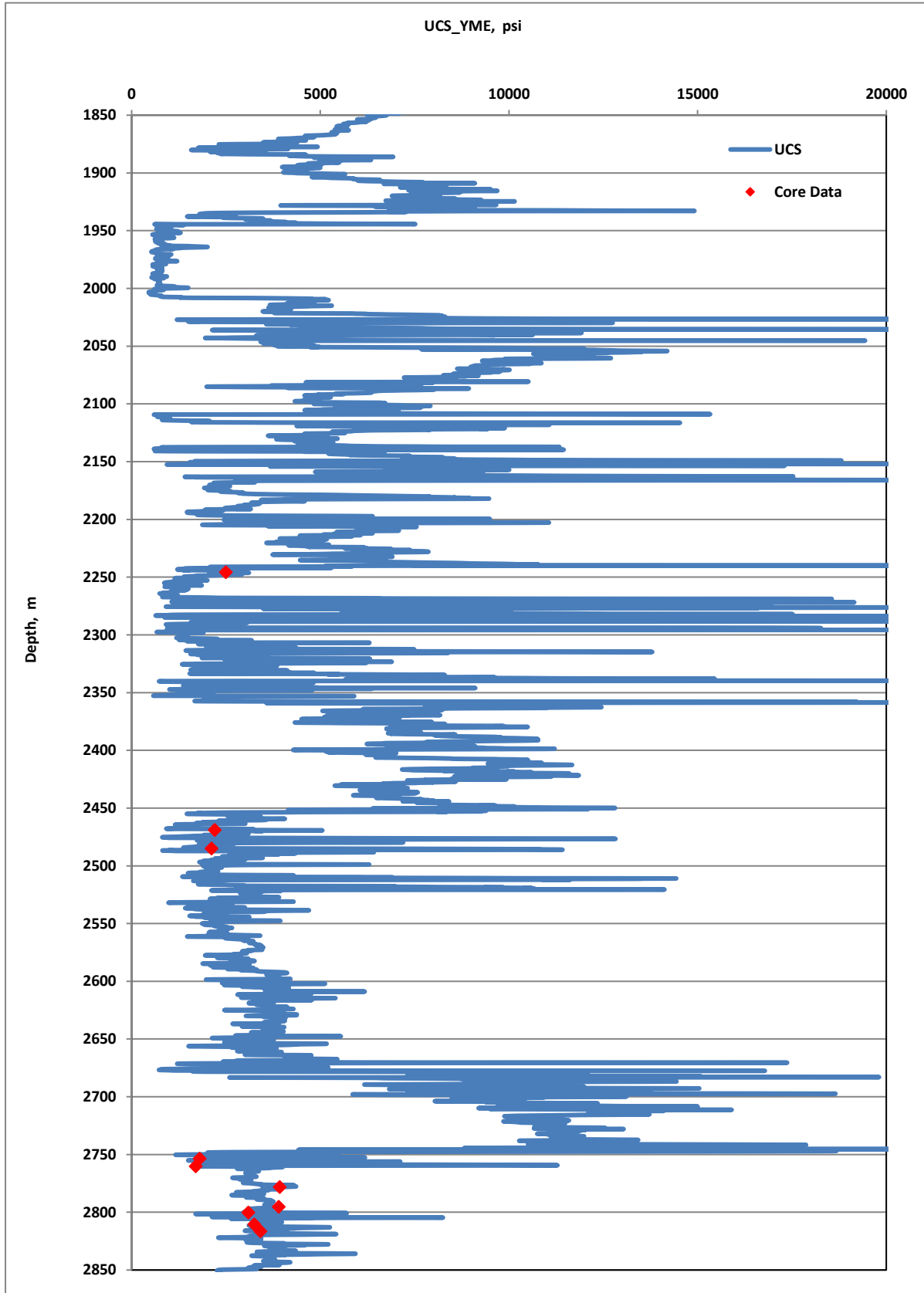


Figure 11. UCS for well X2.

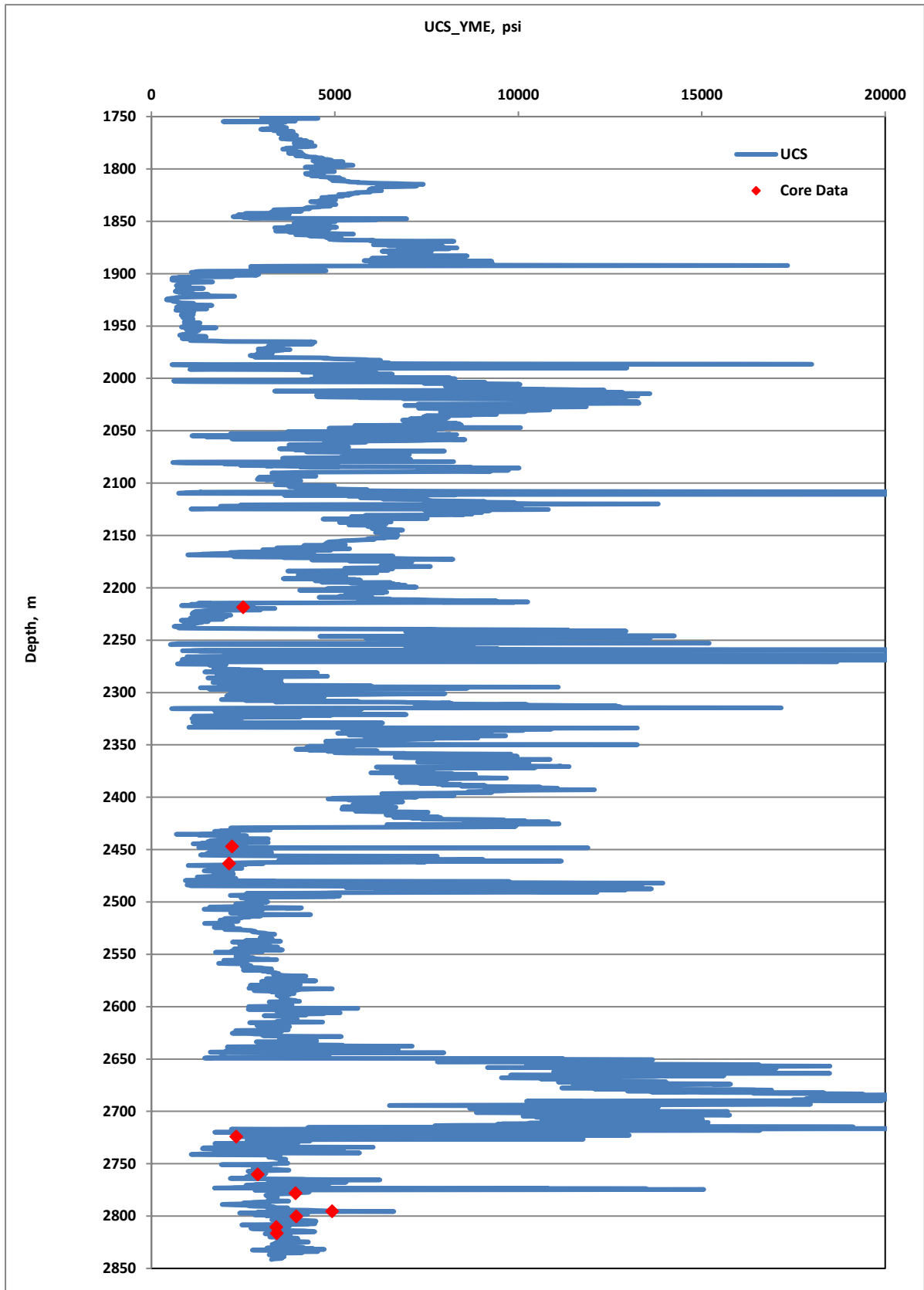


Figure 12. UCS for well X3.

5. STATISTICAL ANALYSIS

Statistical analysis was used to assess the correctness of the projected rock mechanical characteristics based on the empirical correlations described above (**Table 3**). **Fig. 13** depicts the estimated values' root mean square error (RMSE) versus laboratory data. The RMSE was calculated using **Eq. 5**.

$$RMSE = \sqrt{\frac{\sum(x_i - y_i)^2}{n}} \quad (5)$$

where:

X_i is the core-measured value, y_i is estimated value, and n is the number of core-measured values.

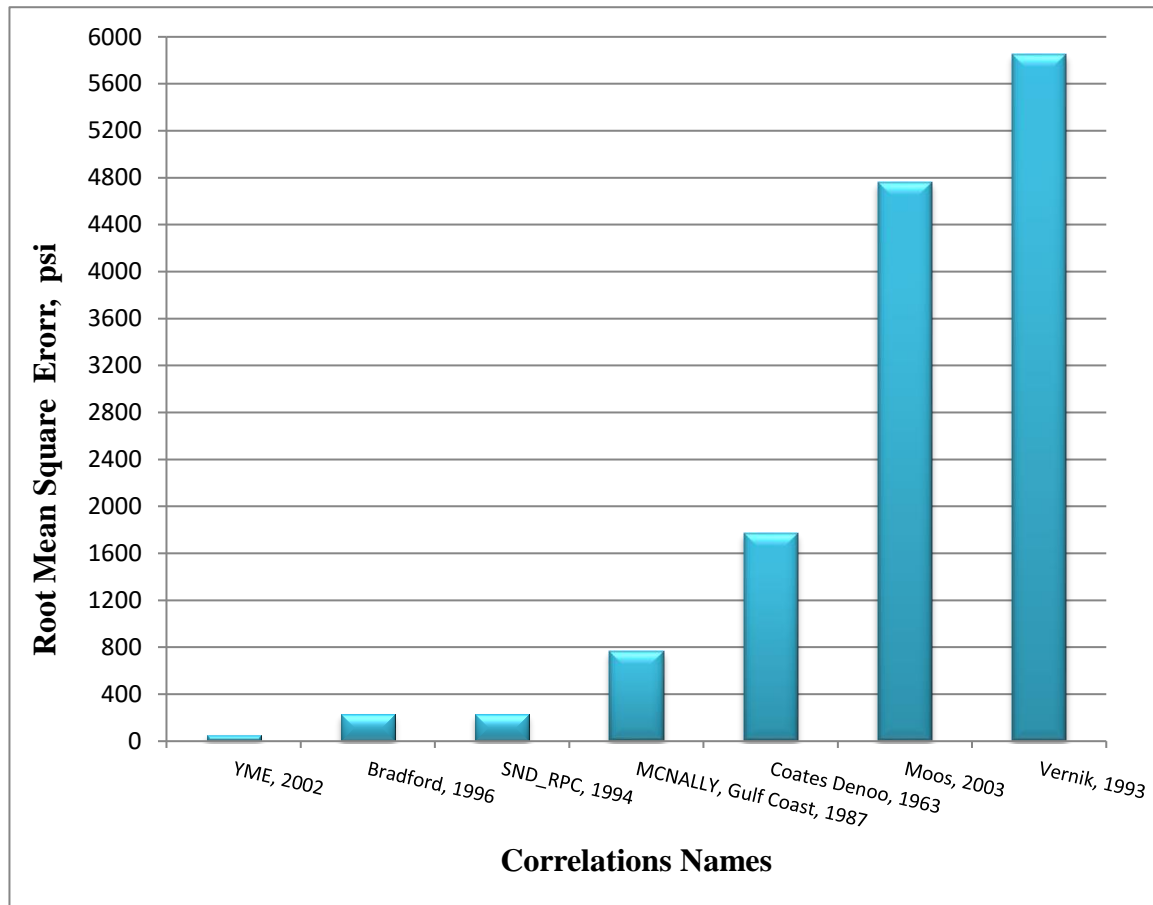


Figure 13. Comparison between results of unconfined compressive strength by different correlations.

Fig. 13 explains that (YME, 2002) gives the least error percentage, and then (Bradford, 1998, SND_RPC) comes, and then (McNally, 1987, Coates Denoo, 1963). While the error percentage increases when the (Moos, 2003, Vernik, 1993) correlations are used.



5. CONCLUSIONS

This work investigates the application of correlations between petrophysical and mechanical properties using wireline log data. The empirical relationships between UCS and E_s with E_d and V_p that previous authors reported were compared with the obtained data. Below are the main conclusions extracted from the discussed results.

- The John Fuller equation (Eq. 2) used to estimate Young's Modulus showed a good match with core tests, so it is recommended to use it in the fields of southern Iraq.
- Estimate the UCS depends on the E_s gives a closer prediction from the actual, contrary to the use of $E_d, \Delta t_c, \phi$, which gives incorrect results.
- The Novel 2021 correlation must be excluded from estimating the UCS because of the large difference between the predicted UCS and core data because this correlation was formulated for shale gas.
- Calculating the UCS based on Young Modulus 2002 correlation in Southern Iraqi fields is recommended. The reason is that this correlation gives a close value to laboratory data (RMSE=53.23psi) regardless of the diversity of the lithology of the section studied from Sadi to Zubair.

ACKNOWLEDGMENTS

This work is supported and carried out in the Department of Petroleum engineering – College of Engineering – University of Baghdad and Thi-Qar Oil Company.

NOMENCLATURE

Symbol	Description	Symbol	Description
E_d	= dynamic Young Modulus, psi.	UCS	= Unconfined compressive strength, psi.
E_s	= static Young Modulus, psi.	ϕ	= Porosity, fraction.
G_{dyn}	= Shear modulus, psi.	Δt_s	= Shear slowness, us/ft.
INOC	= Iraqi national oil company.	Δt_c	= Compressional slowness, us/ft.
K_{dyn}	= Bulk modulus, psi.	ρ	= Bulk density, gm/cc
RMSE	= Root mean square error		

REFERENCES

- Abdulraheem, A., Ahmed, M., Vantala, A., and Parvez, T., 2009. Prediction of rock mechanical parameters for hydrocarbon reservoirs using different artificial intelligence techniques. *SPE Saudi Arabia Section Technical Symposium*. OnePetro. [Doi: 10.2118/126094-MS](https://doi.org/10.2118/126094-MS)
- Ahmed, B. I., and Al-Jawad, M. S., 2020. Geomechanical modelling and two-way coupling simulation for carbonate gas reservoir. *Journal of Petroleum Exploration and Production Technology*, 10, pp. 3619-3648. [Doi: 10.1007/s13202-020-00965-7](https://doi.org/10.1007/s13202-020-00965-7)
- Abed, A. A., and Hamd-Allah, S. M., 2019. Comparative Permeability Estimation Method and Identification of Rock Types using Cluster Analysis from Well Logs and Core Analysis Data in Tertiary Carbonate Reservoir-Khabaz Oil Field. *Journal of Engineering*, 25(12), pp. 49-61. [Doi: 10.31026/j.eng.2019.12.04](https://doi.org/10.31026/j.eng.2019.12.04)
- Al-Shayea, N. A., 2004. Effects of testing methods and conditions on the elastic properties of limestone rock. *Engineering geology*, 74(1-2), pp. 139-156. [Doi: 10.1016/j.enggeo.2004.03.007](https://doi.org/10.1016/j.enggeo.2004.03.007)



- Allawi, R. H., and Al-Jawad, M. S., 2021a. 4D Finite element modeling of stress distribution in depleted reservoir of south Iraq oilfield. *Journal of Petroleum Exploration and Production Technology*, 12, pp. 679-700. Doi: [10.1007/s13202-021-01329-5](https://doi.org/10.1007/s13202-021-01329-5)
- Allawi, R. H., and Al-Jawad, M. S., 2021b. Wellbore instability management using geomechanical modeling and wellbore stability analysis for Zubair shale formation in Southern Iraq. *Journal of Petroleum Exploration and Production Technology*, 11, pp. 4047-4062. Doi: [10.1007/s13202-021-01279-y](https://doi.org/10.1007/s13202-021-01279-y)
- Ameen, M. S., Smart, B. G., Somerville, J. M., Hammilton, S., and Naji, N. A., 2009. Predicting rock mechanical properties of carbonates from wireline logs (A case study: Arab-D reservoir, Ghawar field, Saudi Arabia). *Marine and Petroleum Geology*, 26(4), pp. 430-444. Doi: [10.1016/j.marpetgeo.2009.01.017](https://doi.org/10.1016/j.marpetgeo.2009.01.017)
- Aziz, Q. A. A., and Hussein, H. A., 2021a. Mechanical rock properties estimation for carbonate reservoir using laboratory measurement: A case study from Jeribe, Khasib and Mishrif Formations in Fauqi Oil Field. *The Iraqi Geological Journal*, 21(54), pp. 88-102. Doi: [10.46717/igi.54.1E.8Ms-2021-05-29](https://doi.org/10.46717/igi.54.1E.8Ms-2021-05-29)
- Aziz, Q. A. A., and Hussein, H. A. A., 2021b. Development a Statistical Relationship between Compressional Wave Velocity and Petrophysical Properties from Logs Data for JERIBE Formation ASMARI Reservoir in FAUQI Oil Field. *Iraqi Journal of Chemical and Petroleum Engineering*, 22(3), pp. 1-9. Doi: [10.31699/IJCPE.2021.3.1](https://doi.org/10.31699/IJCPE.2021.3.1)
- Bradford, I., Fuller, J., Thompson, P., and Walsgrove, T., 1998. Benefits of assessing the solids production risk in a North Sea reservoir using elastoplastic modelling. *SPE/ISRM rock mechanics in petroleum engineering*, Trondheim, Norway, July 1998. SPE-47360-MS. doi: [10.2118/47360-MS](https://doi.org/10.2118/47360-MS)
- Chang, C., Zoback, M. D., and Khaksar, A., 2006. Empirical relations between rock strength and physical properties in sedimentary rocks. *Journal of Petroleum Science and Engineering*, 51(3-4), pp. 223-237. Doi: [10.1016/j.petrol.2006.01.003](https://doi.org/10.1016/j.petrol.2006.01.003)
- Edimann, K., Somerville, J., Smart, B., Hamilton, S., and Crawford, B., 1998. Predicting rock mechanical properties from wireline porosities. *SPE/ISRM Rock Mechanics in Petroleum Engineering*. Trondheim, Norway, July 1998. SPE-47344-MS. Doi: [10.2118/47344-MS](https://doi.org/10.2118/47344-MS)
- Fjær, E., Holt, R. M., Horsrud, P., and Raaen, A. M., 2021. *Petroleum related rock mechanics*, Elsevier.
- Hassan, K. H., and Hussien, H. A. A., 2019. Estimation of rock strength from sonic log for Buzurgan oil field: A Comparison study. *Iraqi Journal of Chemical and Petroleum Engineering*, 20(1), pp. 49-52. Doi: [10.31699/IJCPE.2019.1.7](https://doi.org/10.31699/IJCPE.2019.1.7)
- Horsrud, P., 2001. Estimating mechanical properties of shale from empirical correlations. *SPE Drilling & Completion*, 16(2), pp. 68-73. Doi: [10.2118/56017-PA](https://doi.org/10.2118/56017-PA)
- Hoshino, K., 1974. Effect of porosity on the strength of the clastic sedimentary rocks. *Advances in rock mechanics: Proceedings of the 3rd Congress of International Society of Rock Mechanics*, Denver, Colorado, September, pp. 511-516.
- Kowalski, J., 1975. Formation strength parameters from well logs. *SPWLA 16th Annual Logging Symposium*. OnePetro.
- Mcnally, G., 1987. Estimation of coal measures rock strength using sonic and neutron logs. *Geoexploration*, 24(4-5), pp. 381-395. Doi: [10.1016/0016-7142\(87\)90008-1](https://doi.org/10.1016/0016-7142(87)90008-1)
- Neeamy, A. K., and Selman, N. S., 2020. Wellbore breakouts prediction from different rock failure criteria. *Journal of Engineering*, 26(3), pp. 55-64. Doi: [10.31026/j.eng.2020.03.05](https://doi.org/10.31026/j.eng.2020.03.05)



- Onyia, E., 1988. Relationships between formation strength, drilling strength, and electric log properties. SPE Annual Technical Conference and Exhibition. Houston, Texas, Oct. 1988, SPE-18166-MS. [Doi: 10.2118/18166-MS](https://doi.org/10.2118/18166-MS)
- Plumb, R., 1994. Influence of composition and texture on the failure properties of clastic rocks. Rock mechanics in petroleum engineering. OnePetro.
- Ranjbar-Karami, R., and Shiri, M., 2014. A modified fuzzy inference system for estimation of the static rock elastic properties: A case study from the Kangan and Dalan gas reservoirs, South Pars gas field, the Persian Gulf. *Journal of Natural Gas Science and Engineering*, 21, pp. 962-976. [Doi: 10.1016/j.jngse.2014.10.034](https://doi.org/10.1016/j.jngse.2014.10.034)
- Ryshkewitch, E., 1953. Compression strength of porous sintered alumina and zirconia: 9th communication to ceramography. *Journal of the American Ceramic Society*, 36(2), pp. 65-68. [Doi: 10.1111/j.1151-2916.1953.tb12837.x](https://doi.org/10.1111/j.1151-2916.1953.tb12837.x)
- Sarda, J., Kessler, N., Wicquart, E., Hannaford, K., and Deflandre, J., 1993. Use of porosity as a strength indicator for sand production evaluation. SPE Annual Technical Conference and Exhibition. Houston, Texas, Oct. 1993, SPE-26454-MS. [Doi: 10.2118/26454-MS](https://doi.org/10.2118/26454-MS)
- Savitri, C., Maulianda, B., Mohshim, D. & Elraies, K., 2021. A Novel Estimation Approach of Unconfined Compressive Strength (UCS) and Improved Rock Mechanical Properties Correlations by Considering The Effect of Overpressure Condition, Mineralogy, and Shale Composition in Montney Shale Gas, British Columbia, Canada. 55th US Rock Mechanics/Geomechanics Symposium. OnePetro.
- Sethi, D. K., 1981. Well log applications in rock mechanics. SPE/DOE Low Permeability Gas Reservoirs Symposium. OnePetro. [Doi: 10.2118/9833-MS](https://doi.org/10.2118/9833-MS)
- Vernik, L., Bruno, M., and Bovberg, C., 1993. Empirical relations between compressive strength and porosity of siliciclastic rocks. *International journal of rock mechanics and mining sciences & geomechanics abstracts*, 30(7), pp. 677-680. [Doi: 10.1016/0148-9062\(93\)90004-W](https://doi.org/10.1016/0148-9062(93)90004-W)
- Xu, H., Zhou, W., Xie, R., Da, L., Xiao, C., Shan, Y., and Zhang, H., 2016. Characterization of rock mechanical properties using lab tests and numerical interpretation model of well logs. *Mathematical Problems in Engineering*, Article ID 5967159. [Doi: 10.1155/2016/5967159](https://doi.org/10.1155/2016/5967159)